HHS Public Access

Author manuscript

J Thromb Haemost. Author manuscript; available in PMC 2021 November 01.

Published in final edited form as:

J Thromb Haemost. 2020 November ; 18(11): 3078–3085. doi:10.1111/jth.15059.

Injury measurements improve interpretation of thrombus formation data in the cremaster arteriole laser-induced injury model of thrombosis

Steven P Grover[1,2], **Pavan K Bendapudi**[1], **Moua Yang**[1], **Glenn Merrill-Skoloff**[1], **Vijay Govindarajan**[3], **Alexander Y Mitrophanov**[3], **Robert Flaumenhaft**[1]

[1]Division of Hemostasis and Thrombosis and Department of Medicine, Beth Israel Deaconess Medical Center and Harvard Medical School, Boston, Massachusetts, USA

[2]Division of Oncology and Hematology and Department of Medicine, University of North Carolina at Chapel Hill, Chapel Hill, North Carolina, USA

[3]Department of Defense Biotechnology High Performance Computing Software Applications Institute (BHSAI), Telemedicine and Advanced Technology Research Center, U.S. Army Medical Research and Development Command, Fort Detrick, Maryland; The Henry M. Jackson Foundation for the Advancement of Military Medicine, Inc., Bethesda, Maryland, USA

Abstract

Background: The cremaster arteriole laser-induced injury model is a powerful technique with which to investigate the molecular mechanisms that drive thrombus formation. This model is capable of direct visualization and quantification of accumulation of thrombus constituents, including both platelets and fibrin. However, a large degree of variability in platelet accumulation and fibrin formation is observed between thrombi. Strategies to understand this variability will enhance performance and standardization of the model. We determined whether ablation injury size contributes to variation in platelet accumulation and fibrin formation and, if so, whether incorporating ablation injury size into measurements reduces variation.

Methods: Thrombus formation was initiated by laser-induced injury of cremaster arterioles of mice (n=59 injuries). Ablation injuries within the vessel wall were consistently identified and quantified by measuring the length of vessel wall injury observed immediately following laser-induced disruption. Platelet accumulation and fibrin formation as detected by fluorescently-labeled antibodies were captured by digital intra-vital microscopy.

Corresponding author: Robert Flaumenhaft, Division of Hemostasis and Thrombosis, Department of Medicine, Beth Israel Deaconess Medical Center, 330 Brookline Avenue, Boston, MA, 02215, Tel: (617) 754-1204, Fax: (617) 754-1234, rflaumen@bidmc.harvard.edu.

Author Contributions

SPG, GMS, and RF conceived of project and wrote the manuscript. SPG, PKB, MY, and GMS performed experiments and analysed data. SPG, GMS, MY, VG, AYM, and RF contributed to the conceptual development and edited the manuscript.

Publisher's Disclaimer: Disclaimer

The opinions and assertions contained herein are private views of the authors and are not to be construed as official or as reflecting the views of the U.S. Army, the U.S. Department of Defense, or The Henry M. Jackson Foundation for Advancement of Military Medicine, Inc. This article has been approved for public release with unlimited distribution.

Conflict of interest

RF is a founder and consultant for Platelet Diagnostics. The other authors have no conflicts of interest to disclose.

Results: Laser-induced disruption of the vessel wall resulted in ablation injuries of variable length (18–95 μm) enabling interrogation of the relationship between injury severity and thrombus dynamics. Strong positive correlations were observed between vessel injury length and both platelet and fibrin when the data are transformed as area under the curve (Spearman r = 0.80 and 0.76 respectively). Normalization of area under the curve measurements by injury length reduced intraclass coefficients of variation among thrombi and improved hypothesis testing when comparing different data sets.

Conclusions: Measurement of vessel wall injury length provides a reliable and robust marker of injury severity. Injury length can effectively normalize measurements of platelet accumulation and fibrin formation improving data interpretation and standardization.

Keywords

Animal models; Blood Platelets; Fibrin; Thrombosis

Introduction

Thrombosis contributes to myocardial infarction, thrombotic stroke, peripheral vascular disease, deep vein thrombosis, pulmonary embolism, and other pathologies characterized by ischemia and infarction [1–3]. Considerable insight into the mechanisms that drive thrombus formation have been gained from the use of murine models of thrombosis [4, 5]. None of these murine models precisely replicates human thrombosis and most experts agree that use of more than a single model should be employed in evaluating genetically modified animals or new therapeutic interventions [6–8].

The cremaster arteriole laser injury model of thrombosis has been adopted by investigators worldwide [5]. The cremaster arteriole laser injury model uses a focussed laser pulse to cause a localized injury to the vessel wall in cremaster arterioles that serves as a nidus for accumulation of platelets and fibrin [9]. Advantages of the laser-injury model are the ability to control the thrombus in space and time, to generate many thrombi in a single animal, to monitor thrombus kinetics intravitally, and to quantitatively evaluate several thrombus parameters simultaneously. Most of these advantages are also shared by other models of arterial thrombosis such as the mesenteric arteriole ferric chloride model and the femoral artery electrolytic injury model [10–14]. Platelet accumulation, fibrin formation, tissue factor and phosphatidylserine externalization, intraplatelet calcium flux, coagulation factor binding and thrombo-embolization have all been measured using this technology [9, 15–19]. The model has also been used to evaluate the architecture of the platelet mass and to assess the relationship between signalling pathways and clot structure [20, 21].

A major limitation of the laser-injury model of thrombus formation, however, is the significant degree of variability observed among injuries [17, 22, 23]. To overcome the degree of variability observed in the model, investigators typically use large group sizes (~30 injuries per group). Nonetheless, large variance within a group frequently limits conclusions when comparing different conditions. Although acknowledged as a significant problem, the sources of the variability in this model are poorly understood. We postulated that ablation injury size following laser injury is a significant determinant of thrombus size. We sought to

determine the extent to which variation in the severity of vessel wall injury contributes to observed variance in thrombus formation in the cremaster arteriole laser injury model by measuring injury length in this model and determining its correlation to platelet and fibrin accumulation.

Methods

Cremaster arteriole laser injury model

Male 8-10 week old C57BL6/J mice (Strain # 000664, Jackson Laboratory, ME) were anesthetized with a ketamine and xylazine cocktail administered by intraperitoneal injection. An indwelling catheter was placed in the jugular vein to allow for further intravenous administration of ketamine to maintain the mouse in an appropriate plane of anesthesia and for subsequent administration of fluorescently labelled antibodies. A testis was externalized from the scrotum and secured to a custom intravital imaging tray using a 28G needle (Fig S1A). Excess connective tissue and fat was removed from the testis using a pair of fine tipped forceps. An incision was made in the cremaster muscle extending proximally from the base of the testis allowing the cremaster muscle to be pinned out over a cover slip mounted in the intravital imaging tray. The cremaster muscle was superperfused with 37°C bicarbonate buffered saline aerated with 95% N_2, 5% CO_2. Mice were administered Dylight647 labeled anti-CD42b (0.1 mg/g body weight; Emfret, Germany) or Dylight488 labeled anti-fibrin (clone 59D8, 0.5 mg/g body weight) by intravenous infusion through the indwelling jugular catheter.

Cremaster arterioles were subject to injury using a 170 μJ pulsed nitrogen dye laser (peak power 45 kW, average power 3 mW) at 440 nm using the Micropoint laser system (Andor, Belfast, UK). The pulse was directed at a point just inside the lumen of the vessel adjacent to the vessel wall. Each pulse of the laser lasted 3 to 5 ns and had a near diffraction-limited spot size (~270 nm). For each laser injury location, the laser was fired at four points in a two by two matrix with 500 nm spacing between each pulse. This pattern was repeated six times for a total of 24 continuous pulses per ablation at a frequency of 20 pulses per second. The power of each laser pulse at the site of injury cannot be measured directly, however, based on the power of the laser source of 170 μJ, estimated attenuation of approximately 97-98% by the microscope, and estimated attenuation by connective tissue of the cremaster tissue (approximately 20-40%), we calculate that approximately 40-74 $\mu J/\mu m^2$ is delivered to the site of injury as a 3.5 nanosecond pulse that equates to 11 to 21 $kJ/\mu m^2/s$. Vascular injury in the cremaster arteriole laser injury model is thought to occur through laser injury mediated activation of the endothelium [16]. The absence of detectable levels of subendothelial collagen exposure indicates that this model does not result in endothelial denudation [24]. The percentage power of the laser pulse applied was adjusted to cause an injury that resulted in distortion of the vessel wall (as shown in Fig. S2) and formation of a non-occlusive platelet thrombus. In this model the power of the laser pulse applied frequently needs adjustment to accommodate for differences in thickness of the cremaster muscle and size of the arteriole. Accumulation of fluorescent signal at the site of thrombus was visualized through a 60x 1.0 NA water immersion objective (Olympus, Japan) mounted to an AX-70 fluorescence microscope (Olympus Japan) equipped with a CCD camera (ORCA Flash 4.0,

Hamamatsu Photonics, Japan). Images were captured in three channels (Brightfield, 488/520 nm and 640/670 nm) for 240 seconds at 2 frames/second using a digital camera. Data acquisition and analysis were conducted using SlideBook software (v6.0, Intelligent Imaging Innovations, CO). Injuries in which excessive extravasation of erythrocytes was observed (greater than 10 erythrocytes) or in which the vessel became occluded for greater than 5 seconds were excluded from subsequent analyses. Data of 1-aminobenzotriazole pretreated C57BL6/J mice (n=3-4 per group) treated with bepristat 2a (15 mg/kg) or vehicle control administered intravenously immediately prior to the first injury was also analyzed [25].

Statistical Analysis

The data were analyzed under non-parametric conditions unless otherwise stated. In studies correlating injury length and platelet and fibrin accumulation, Spearman correlations were performed. To assess the reproducibility of injury length measurements intraclass correlation coefficients were conducted. *P*-values of <0.05 were considered statistically significant.

Measurement of ablation injury length in the cremaster arteriole laser injury model

Ablation injuries were observable by white-light trans illumination of the cremaster muscle, presenting as a distortion of the vessel wall in the region adjacent to the injury site. This distortion was quantified by measuring the length of the disrupted region in micrometers. Using the Slidebook software package (Intelligent Imaging Innovations, CO.), we digitally captured data every 0.5 seconds in the trans-illuminated channel, as well as in epi-illuminated fluorescent channels. This approach allowed us to quantify the length of the disrupted region along the luminal face in the frames following injury. Although we found that this length remains constant after the initial ablative event, we made all our measurements in the frame immediately following injury for consistency. These measurements were exported and further analysed with statistical software (Excel, Microsoft, WA; Prism v8, Graphpad, CA or SPSS Statistics v26, IBM, NY).

Results

Injuries were induced along the cremaster vasculature of the mouse arteriole by laser injury. Multiple injuries were performed in each of five mice and were made either upstream from the previous injury or on different branches of the arteriole vascular tree (Figs. S1B and S1C). To assess the variability observed in this model, platelet and fibrin accumulation were determined in 59 injuries. Fluorescence intensity values for platelet accumulation (λ_{ex} = 647) and fibrin accumulation (λ_{ex} = 488) were plotted over time. An overlay of the platelet and fibrin accumulation tracings for all 59 thrombi demonstrated the substantial variability of these data (Figs. S1D and S1E). A median curve derived from the 59 individual tracings was generated by taking the median platelet or fibrin fluorescence values of the 59 thrombi at each 0.5 second time point (Figs. S1F and S1G). To provide an overall measure of thrombus size, area under the curve (AUC) measurements were made for each thrombus (Figs. S1H and S1I). Such measurements reflect the overall accumulation of platelets and fibrin during the time course of thrombus formation. It is important to note that platelet AUC measurements provide a single measure that integrates the dynamic accumulation,

disintegration and reaccumulation of the platelet mass at the site of injury. Figs. S1J and S1K illustrate the means and distribution of the AUC data in each parameter. Both platelet and fibrin accumulation were significantly non-normal in this data set as assessed by Pearson D'agostino normality tests ($P<0.05$), with histograms demonstrating a marked degree of skew and curtosis (Figs. S1L and S1M). Coefficients of variation (CoV), a measure of variability within a single dataset, were 120% and 66% for platelet and fibrin AUCs, respectively.

Laser-induced injury resulted in the formation of a region of vascular disruption. This region of vascular disruption appeared as a distortion of the vessel wall adjacent to the site of laser injury (Figs. 1A–C; Fig. S2A). To establish a quantitative measure of injury severity, the length of the region of vascular disruption in contact with the vessel lumen was determined and is referred to as the laser ablation injury length (Figs. 1A–C). This laser ablation injury length varied markedly between injuries, ranging between roughly 20 μm and 100 μm, and resulted in different sized thrombi (Fig. 1). Measurements of laser ablation injury length was similar between two blinded investigators and demonstrated a normal distribution (Fig. S2). A strong agreement between investigator measurements was observed by intraclass correlation coefficient analysis (ICC=0.87, $P<0.0001$). To evaluate the relationship between injury severity and the dynamics of thrombus formation, platelet accumulation and fibrin generation were plotted as a function of injury length (Figs. 1J–M). A highly significant positive correlation was observed between injury length and platelet accumulation represented by AUC measurements (Spearman $r = 0.80$, $P<0.0001$, Fig. 1J). Similarly, a strong positive correlation was observed between injury length and fibrin accumulation represented by AUC measurements (Spearman $r = 0.76$, $P<0.0001$, Fig. 1K). A strong correlation was also observed between injury size and measurements of peak platelet accumulation (Spearman $r = 0.76$, $P<0.0001$, Fig 1L) and fibrin accumulation (Spearman $r = 0.66$, $P<0.0001$, Fig 1M).

Based on the non-linear relationship between platelet accumulation and injury length, non-linear regression lines were fitted to plots of injury length vs platelet AUC ($y=1x10^9(e^{0.0593x})$, Fig. 1J) and injury length vs fibrin AUC ($y=3x10^9(e^{0.0337x})$, Fig. 1K). The calculated regression lines demonstrated a good level of agreement with the experimental data for both platelet AUC ($R^2 = 0.63$) and fibrin AUC ($R^2 = 0.58$). To determine if injury length could serve as a normalizing factor for the measures of platelet and fibrin accumulation, we transformed platelet and fibrin AUC measurements, dividing individual AUC values by their corresponding injury length. This normalization resulted in a reduction in the observed coefficients of variation for both platelet AUC and fibrin AUC by 15% (i.e., from 120% to 101%) and 30% (i.e., from 66% to 47%), respectively. These data demonstrate that platelet and fibrin accumulation vary directly with injury length and that normalization based on injury length decreases variance among injuries obtained under a single condition.

Differences in the cremaster preparation and other variables can result in differences in thrombus size even among genetically identical mice. One potential benefit of correcting for injury size is to decrease this variation. Analysis of a group of C57BL6/J mice ($n = 5$) demonstrated differences in platelet accumulation, fibrin accumulation, and ablation injury

length among the mice (Figs. 2A–C). A plot of platelet accumulation (Fig. 2D) and fibrin accumulation (Fig. 2E) as a function of injury length demonstrated that mice with smaller injuries (e.g., mouse 1) had less platelet accumulation and fibrin accumulation than mice with larger injuries (e.g., mouse 4). Interestingly, there was some disconnect in the relationship between injury size and platelet or fibrin accumulation when comparing individual mice. For example, a marked difference in median platelet and fibrin between mouse 2 and mouse 3 (Figs. 2A and B) was observed despite the fact that median injury size was roughly equivalent in these two mice (Fig 2C). Dividing the AUC values by injury length (Figs. 2F and G) decreased the variance among fluorescence values obtained from each mouse as indicated by the decrease in the CoV (Table S1). Normalizing data by dividing fluorescence by injury length also reduced differences in median values. The CoVs calculated for the median fluorescence values obtained from the five mice decreased after normalization by injury length when evaluating platelet accumulation (pre-normalization CoV: 73.7%, post-normalization CoV: 65.2%) and fibrin accumulation (pre-normalization CoV: 54.9%, post-normalization CoV: 37.8%).

To test the utility of incorporating injury size into an evaluation of a potential antithrombotic, we determined how fibrin accumulation following laser injury was influenced by bepristat 2a, a protein disulfide isomerase inhibitor previously shown to inhibit platelet accumulation [25]. Specifically, we compared a data set of thrombi obtained in one set of mice following infusion of DMSO alone to a data set of thrombin obtained in a second set of mice following infusion of bepristat 2a and performed measurements of both fibrin accumulation and injury length. The uncorrected data set showed 47.0% inhibition of fibrin accumulation with bepristat 2a, but did not reach statistical significance based on the variance ($P > 0.05$, Fig. S3A). Measurement of injury lengths showed that there was no significant difference between groups ($P = 0.79$; Fig. S3B). However, when AUC was normalized for injury length in both data sets, the difference between the DMSO control and the bepristat 2a condition increased to 52.5% inhibition and the difference became statistically significant ($P = 0.027$; Fig. S3C). The normalized data indicate that bepristat 2a inhibits fibrin accumulation following laser injury.

Discussion

This study demonstrates that laser ablation injury length in the cremaster arteriole model correlates directly with accumulation of platelets and fibrin (Fig. 1). Laser injury in the cremaster arteriole model resulted in a region of vascular disruption, consistent with observations by others in laser induced injury models [24, 26–29]. Unlike the previous report of Hechler and colleagues [26], however, we observed a significant degree of variability - nearly fivefold - in the length of the region of vascular disruption (Fig. S2B). The variability in injury size is an important observation and explains some of the large variability in platelet and fibrin accumulation observed in the cremaster arteriole laser injury model. It is intuitively clear that thrombus size should vary with injury size; however, there are several potential applications of this simple measurement that warrant consideration.

Interpretation of thrombus formation data is improved by inclusion of injury length measurements. Calculating platelet and fibrin AUC measurements as a direct function of

injury length markedly reduced the observed CoV when compared with fluorescence measurements alone. Normalization of fibrin accumulation by injury size resulted in a more marked reduction in the coefficient of variance than normalization of platelet accumulation likely owing to the more linear relationship between fibrin accumulation and injury size. Normalization of thrombus formation measurements as a function of injury length also modified the mean platelet and fibrin fluorescence. In the case of comparing genetically identical mice, incorporation of ablation injury length measurements brought the means of individual mice closer together (Fig. 2), indicating that differences in injury size contributed to differences in platelet accumulation and fibrin accumulation. Differences in injury size could result from the surgical preparations as these vary somewhat from mouse to mouse. For example, the amount of residual connective tissue left associated with the blood vessel or other cross-vessel structures could impact the light path of the laser, thereby affecting injury size and contributing to differences in thrombus size between genetically identical mice. Normalization by injury length improves interpretation of fluorescence measurements by correcting for variables that contribute to differences in ablation injury size.

The evaluation of mechanisms of thrombus formation can also be improved by consideration of injury severity. The work of Welsh and colleagues used severe laser injury of cremaster arterioles to investigate the contribution of platelets to vascular sealing in response to penetrating vascular injury [30]. The contribution of specific proteins or pathways to thrombus formation can vary depending on injury size, making injury size a relevant consideration in assessing mechanism. In a mesenteric arteriole laser injury model, Nonne et al. found that deletion of phospholipase Cγ2 impaired thrombus formation in superficial lesions, but not in more severe lesions, whereas Gαq deletion inhibited thrombus formation in both lesion types [28]. Similarly, deletion of vWF strongly blunted thrombus formation after both superficial and severe injuries, but immunodepletion of glycoprotein VI, selectively blunted thrombus formation in superficial injuries [26]. We have found that separation of data by ablation injury measurements revealed a differential effect of tissue factor between small and large injuries (Sol Schulman, personal communication). By segregating data by injury severity using measurements of injury length, investigators can identify previously undetected differential effects of coagulation and platelet proteins in thrombi of different sizes.

Standardization and quality control of the laser induced injury model could also be improved by consideration of ablation injury size. Unlike fluorescence measurements, which are reported as relative fluorescence units and vary between different laboratories because of differences in microscopy set-up, camera types, and antibody specificities and batches, ablation injury length provides an absolute measurement in microns. This measurement can be compared among different users within a laboratory to ensure uniformity of technique and enable comparisons between laboratories to determine if different laboratories are inducing similar injury lengths. Other investigators have used different laser pulse frequencies and pulse numbers to modulate injury severity [26]. The findings of this study may not extrapolate to those in which prolonged injury protocols are used. However, the approach described herein offers a useful endpoint measurement that has the potential to facilitate cross study comparison when different methods of laser injury induction are used. Determining whether ablation injury length differs between the control and experimental

data sets can be a useful quality control measure. Such evaluation can determine whether observed differences in thrombus formation result from differences in injury length or thrombus formation *per se*. Normalization of fluorescence measurements by ablation injury length will help decrease variability both within and among laboratories using the cremaster laser injury model. If this method could be applied to other laser injury models (e.g. the mesenteric artery model) requires further investigation.

It is important to note, however, that a significant proportion of the observed variability cannot be accounted for by injury size alone. Indeed, a disconnect between injury size and platelet or fibrin accumulation was observed between some mice. Further, differences between injuries and between mice were still apparent after normalization. It is likely that additional factors, such as vessel geometry, contribute to the observed variation. Variation in blood flow within and between arteriole beds, vascular responsiveness, and vessel anatomy could all affect fluid dynamics at the site of injury and contribute to variability [31, 32]. Changes in blood flow would likely alter vessel wall shear stress which is a critical regulator of platelet activation and accumulation [33, 34]. While it is also possible that serial injuries of a single arteriole could affect thrombus formation, we have not observed an impact of distal injuries on platelet or fibrin accumulation on subsequent proximal injuries [35, 36]. Differences in residual connective tissue will also affect the path of fluorescence light and is a variable not accounted for by ablation injury size. Furthermore, the specific mechanism of the vascular disruption is unclear. This work has focussed on the relationship between vessel injury size and area under the curve measurements for fibrin and platelets. Area under the curve measurements provide a useful measure of thrombus burden over a defined time period. Further work is required to determine if normalization is effective for other parameters of thrombus formation.

Taken together our data demonstrate that ablation injury size is an important determinant of platelet and fibrin accumulation in the cremaster arteriole laser injury model. Measurement of ablation size is determined by standard brightfield microscopy and is readily applicable to any laboratory that uses the cremaster laser injury ablation model for assessment of thrombus formation. Normalizing data to measurements of ablation injury size by dividing fluorescence measurement by injury size can correct for the considerable variability in this model and improve data interpretation. Furthermore, measurements of injury size may also prevent the introduction of unintentional bias by ensuring equivalent injury severities between control and experimental groups. We contend that measurements of injury length should be routinely incorporated into the analysis of thrombi in the cremaster arteriole laser injury model.

Supplementary Material

Refer to Web version on PubMed Central for supplementary material.

Acknowledgments

Funding

This work was funded by the National Heart, Lung, and Blood Institute (Grants R01HL125275, R35HL135775, and T32 HL007917 to RF). The work of VG and AYM was supported by the U.S. Army Medical Research and Development Command, Fort Detrick, Maryland. SPG is supported by a postdoctoral fellowship from the American Heart Association (19POST34370026).

References

1. Lippi G, Franchini M, Targher G. Arterial thrombus formation in cardiovascular disease. Nat Rev Cardiol. 2011; 8: 502–12. 10.1038/nrcardio.2011.91. [PubMed: 21727917]
2. Wolberg AS, Rosendaal FR, Weitz JI, Jaffer IH, Agnelli G, Baglin T, Mackman N. Venous thrombosis. Nat Rev Dis Primers. 2015; 1: 15006 10.1038/nrdp.2015.6. [PubMed: 27189130]
3. Raskob G, Angchaisuksiri P, Blanco A, Buller H, Gallus A, Hunt B, Hylek E, Kakkar A, Konstantinides S, McCumber M, Ozaki Y, Wendelboe A, Weitz J. Thrombosis: a major contributor to the global disease burden. Journal of Thrombosis and Haemostasis. 2014; 12: 1580–90. [PubMed: 25302663]
4. Westrick RJ, Winn ME, Eitzman DT. Murine models of vascular thrombosis (Eitzman series). Arterioscler Thromb Vasc Biol. 2007; 27: 2079–93. 10.1161/ATVBAHA.107.142810. [PubMed: 17600224]
5. Jackson SP. Arterial thrombosis--insidious, unpredictable and deadly. Nat Med. 2011; 17: 1423–36. 10.1038/nm.2515. [PubMed: 22064432]
6. Jagadeeswaran P, Cooley BC, Gross PL, Mackman N. Animal Models of Thrombosis From Zebrafish to Nonhuman Primates: Use in the Elucidation of New Pathologic Pathways and the Development of Antithrombotic Drugs. Circ Res. 2016; 118: 1363–79. 10.1161/CIRCRESAHA.115.306823. [PubMed: 27126647]
7. Diaz JA, Saha P, Cooley B, Palmer OR, Grover SP, Mackman N, Wakefield TW, Henke PK, Smith A, Lal BK. Choosing a Mouse Model of Venous Thrombosis. Arterioscler Thromb Vasc Biol. 2019: ATVBAHA118311818. 10.1161/ATVBAHA.118.311818.
8. Diaz JA, Saha P, Cooley B, Palmer OR, Grover SP, Mackman N, Wakefield TW, Henke PK, Smith A, Lal BK. Choosing a mouse model of venous thrombosis: a consensus assessment of utility and application. J Thromb Haemost. 2019; 17: 699–707. 10.1111/jth.14413. [PubMed: 30927321]
9. Falati S, Gross P, Merrill-Skoloff G, Furie BC, Furie B. Real-time in vivo imaging of platelets, tissue factor and fibrin during arterial thrombus formation in the mouse. Nat Med. 2002; 8: 1175–81. 10.1038/nm782. [PubMed: 12244306]
10. Ni H, Denis CV, Subbarao S, Degen JL, Sato TN, Hynes RO, Wagner DD. Persistence of platelet thrombus formation in arterioles of mice lacking both von Willebrand factor and fibrinogen. J Clin Invest. 2000; 106: 385–92. 10.1172/JCI9896. [PubMed: 10930441]
11. Reheman A, Gross P, Yang H, Chen P, Allen D, Leytin V, Freedman J, Ni H. Vitronectin stabilizes thrombi and vessel occlusion but plays a dual role in platelet aggregation. J Thromb Haemost. 2005; 3: 875–83. 10.1111/j.1538-7836.2005.01217.x. [PubMed: 15733060]
12. Reheman A, Yang H, Zhu G, Jin W, He F, Spring CM, Bai X, Gross PL, Freedman J, Ni H. Plasma fibronectin depletion enhances platelet aggregation and thrombus formation in mice lacking fibrinogen and von Willebrand factor. Blood. 2009; 113: 1809–17. 10.1182/blood-2008-04-148361. [PubMed: 19036705]
13. Cooley BC. In vivo fluorescence imaging of large-vessel thrombosis in mice. Arterioscler Thromb Vasc Biol. 2011; 31: 1351–6. 10.1161/ATVBAHA.111.225334. [PubMed: 21393581]
14. Aleman MM, Walton BL, Byrnes JR, Wang JG, Heisler MJ, Machlus KR, Cooley BC, Wolberg AS. Elevated prothrombin promotes venous, but not arterial, thrombosis in mice. Arterioscler Thromb Vasc Biol. 2013; 33: 1829–36. 10.1161/ATVBAHA.113.301607. [PubMed: 23723374]
15. Falati S, Liu Q, Gross P, Merrill-Skoloff G, Chou J, Vandendries E, Celi A, Croce K, Furie BC, Furie B. Accumulation of tissue factor into developing thrombi in vivo is dependent upon microparticle P-selectin glycoprotein ligand 1 and platelet P-selectin. J Exp Med. 2003; 197: 1585–98. 10.1084/jem.20021868. [PubMed: 12782720]
16. Atkinson BT, Jasuja R, Chen VM, Nandivada P, Furie B, Furie BC. Laser-induced endothelial cell activation supports fibrin formation. Blood. 2010; 116: 4675–83. 10.1182/blood-2010-05-283986. [PubMed: 20675401]

17. Dubois C, Panicot-Dubois L, Gainor JF, Furie BC, Furie B. Thrombin-initiated platelet activation in vivo is vWF independent during thrombus formation in a laser injury model. J Clin Invest. 2007; 117: 953–60. 10.1172/JCI30537. [PubMed: 17380206]

18. Stolla M, Stefanini L, Roden RC, Chavez M, Hirsch J, Greene T, Ouellette TD, Maloney SF, Diamond SL, Poncz M, Woulfe DS, Bergmeier W. The kinetics of αIIbβ3 activation determines the size and stability of thrombi in mice: implications for antiplatelet therapy. Blood. 2011; 117: 1005–13. 10.1182/blood-2010-07-297713. [PubMed: 20971951]

19. Ivanciu L, Krishnaswamy S, Camire RM. New insights into the spatiotemporal localization of prothrombinase in vivo. Blood. 2014; 124: 1705–14. 10.1182/blood-2014-03-565010. [PubMed: 24869936]

20. Stalker TJ, Traxler EA, Wu J, Wannemacher KM, Cermignano SL, Voronov R, Diamond SL, Brass LF. Hierarchical organization in the hemostatic response and its relationship to the platelet-signaling network. Blood. 2013; 121: 1875–85. 10.1182/blood-2012-09-457739. [PubMed: 23303817]

21. Stalker TJ, Welsh JD, Tomaiuolo M, Wu J, Colace TV, Diamond SL, Brass LF. A systems approach to hemostasis: 3. Thrombus consolidation regulates intrathrombus solute transport and local thrombin activity. Blood. 2014; 124: 1824–31. 10.1182/blood-2014-01-550319. [PubMed: 24951426]

22. Shen J, Sampietro S, Wu J, Tang J, Gupta S, Matzko CN, Tang C, Yu Y, Brass LF, Zhu L, Stalker TJ. Coordination of platelet agonist signaling during the hemostatic response in vivo. Blood Adv. 2017; 1: 2767–75. 10.1182/bloodadvances.2017009498. [PubMed: 29296928]

23. Vandendries ER, Hamilton JR, Coughlin SR, Furie B, Furie BC. Par4 is required for platelet thrombus propagation but not fibrin generation in a mouse model of thrombosis. Proc Natl Acad Sci U S A. 2007; 104: 288–92. 10.1073/pnas.0610188104. [PubMed: 17190826]

24. Dubois C, Panicot-Dubois L, Merrill-Skoloff G, Furie B, Furie BC. Glycoprotein VI-dependent and -independent pathways of thrombus formation in vivo. Blood. 2006; 107: 3902–6. 10.1182/blood-2005-09-3687. [PubMed: 16455953]

25. Bekendam RH, Bendapudi PK, Lin L, Nag PP, Pu J, Kennedy DR, Feldenzer A, Chiu J, Cook KM, Furie B, Huang M, Hogg PJ, Flaumenhaft R. A substrate-driven allosteric switch that enhances PDI catalytic activity. Nat Commun. 2016; 7: 12579 10.1038/ncomms12579. [PubMed: 27573496]

26. Hechler B, Nonne C, Eckly A, Magnenat S, Rinckel JY, Denis CV, Freund M, Cazenave JP, Lanza F, Gachet C. Arterial thrombosis: relevance of a model with two levels of severity assessed by histologic, ultrastructural and functional characterization. J Thromb Haemost. 2010; 8: 173–84. 10.1111/j.1538-7836.2009.03666.x. [PubMed: 19874458]

27. Rosen ED, Raymond S, Zollman A, Noria F, Sandoval-Cooper M, Shulman A, Merz JL, Castellino FJ. Laser-induced noninvasive vascular injury models in mice generate platelet- and coagulation-dependent thrombi. Am J Pathol. 2001; 158: 1613–22. 10.1016/S0002-9440(10)64117-X. [PubMed: 11337359]

28. Nonne C, Lenain N, Hechler B, Mangin P, Cazenave JP, Gachet C, Lanza F. Importance of platelet phospholipase Cgamma2 signaling in arterial thrombosis as a function of lesion severity. Arterioscler Thromb Vasc Biol. 2005; 25: 1293–8. 10.1161/01.ATV.0000163184.02484.69. [PubMed: 15774906]

29. Ivanciu L, Stalker TJ. Spatiotemporal regulation of coagulation and platelet activation during the hemostatic response in vivo. J Thromb Haemost. 2015; 13: 1949–59. 10.1111/jth.13145. [PubMed: 26386264]

30. Welsh JD, Muthard RW, Stalker TJ, Taliaferro JP, Diamond SL, Brass LF. A systems approach to hemostasis: 4. How hemostatic thrombi limit the loss of plasma-borne molecules from the microvasculature. Blood. 2016; 127: 1598–605. 10.1182/blood-2015-09-672188. [PubMed: 26738537]

31. Cosemans JM, Angelillo-Scherrer A, Mattheij NJ, Heemskerk JW. The effects of arterial flow on platelet activation, thrombus growth, and stabilization. Cardiovasc Res. 2013; 99: 342–52. 10.1093/cvr/cvt110. [PubMed: 23667186]

32. Lei X, Reheman A, Hou Y, Zhou H, Wang Y, Marshall AH, Liang C, Dai X, Li BX, Vanhoorelbeke K, Ni H. Anfibatide, a novel GPIb complex antagonist, inhibits platelet adhesion and thrombus

formation in vitro and in vivo in murine models of thrombosis. Thromb Haemost. 2014; 111: 279–89. 10.1160/TH13-06-0490. [PubMed: 24172860]

33. Nesbitt WS, Westein E, Tovar-Lopez FJ, Tolouei E, Mitchell A, Fu J, Carberry J, Fouras A, Jackson SP. A shear gradient-dependent platelet aggregation mechanism drives thrombus formation. Nat Med. 2009; 15: 665–73. 10.1038/nm.1955. [PubMed: 19465929]
34. Ruggeri ZM, Orje JN, Habermann R, Federici AB, Reininger AJ. Activation-independent platelet adhesion and aggregation under elevated shear stress. Blood. 2006; 108: 1903–10. 10.1182/blood-2006-04-011551. [PubMed: 16772609]
35. Celi A, Merrill-Skoloff G, Gross P, Falati S, Sim DS, Flaumenhaft R, Furie BC, Furie B. Thrombus formation: direct real-time observation and digital analysis of thrombus assembly in a living mouse by confocal and widefield intravital microscopy. J Thromb Haemost. 2003; 1: 60–8. 10.1046/j.1538-7836.2003.t01-1-00033.x. [PubMed: 12871540]
36. Sim DS, Merrill-Skoloff G, Furie BC, Furie B, Flaumenhaft R. Initial accumulation of platelets during arterial thrombus formation in vivo is inhibited by elevation of basal cAMP levels. Blood. 2004; 103: 2127–34. 10.1182/blood-2003-04-1133. [PubMed: 14645013]

Essentials

- The cremaster arteriole laser injury model is a powerful tool to study mechanisms of thrombosis
- This model is associated with a significant degree of variability between injuries
- Injury size strongly correlated with measurements of platelet and fibrin accumulation
- Normalizing platelet or fibrin accumulation to injury size reduced coefficients of variance

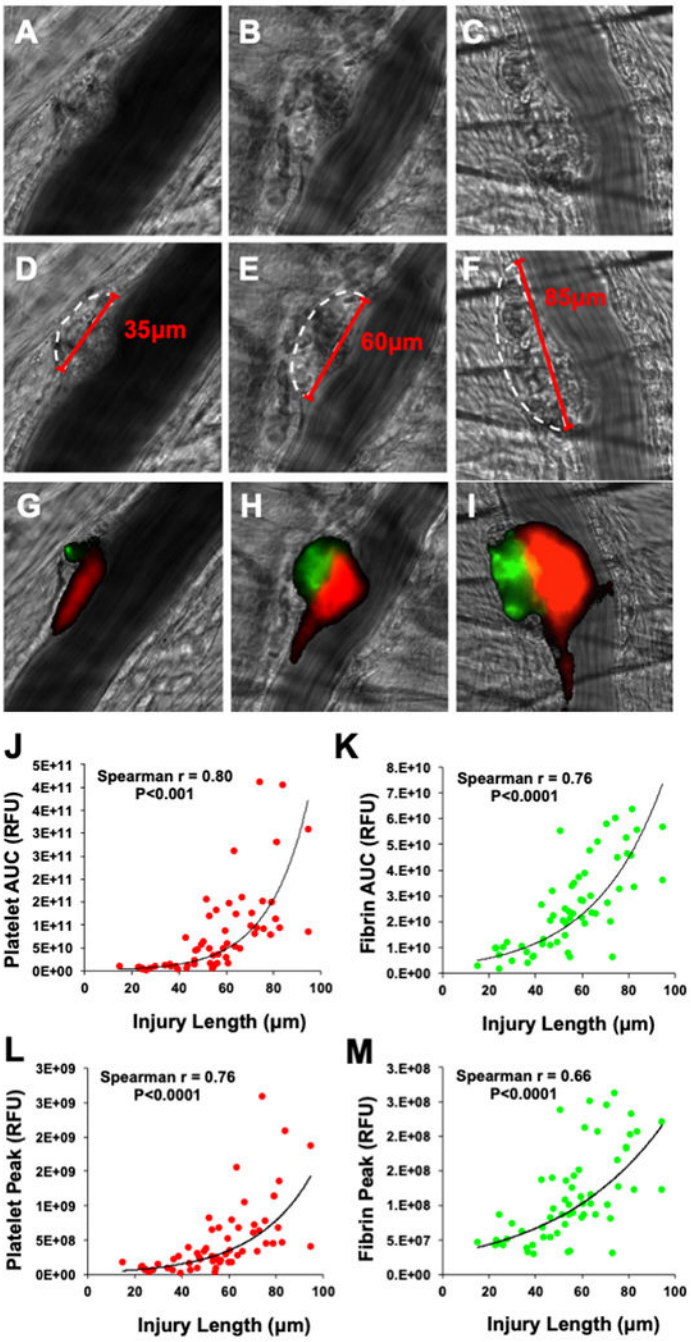

Figure 1: Normalizing to injury size reduces platelet and fibrin coefficients of variation.

(A-C) Brightfield images of the cremaster arteriole immediately following laser induced injury were used to identify the region of vascular disruption (white dotted outline). The size of the region of vascular injury in contact with the vessel lumen was then determined (red line) allowing for quantitative measures of injury size to be made. An apparent correlation between the size of vessel injury observed in (D-F) brightfield images and the resultant accumulation of (H-I) platelets and fibrin was detected. (J) Injury size when plotted against the platelet area under the curve (AUC) measurements revealed a strong positive correlation

(Spearman rank, P<0.0001). (K) Similarly, when injury size was plotted against the fibrin AUC measurements, a strong positive correlation was also observed (Spearman rank, P<0.0001). Strong positive correlations were also observed between injury size and (L) peak platelet accumulation and (M) peak fibrin accumulation.

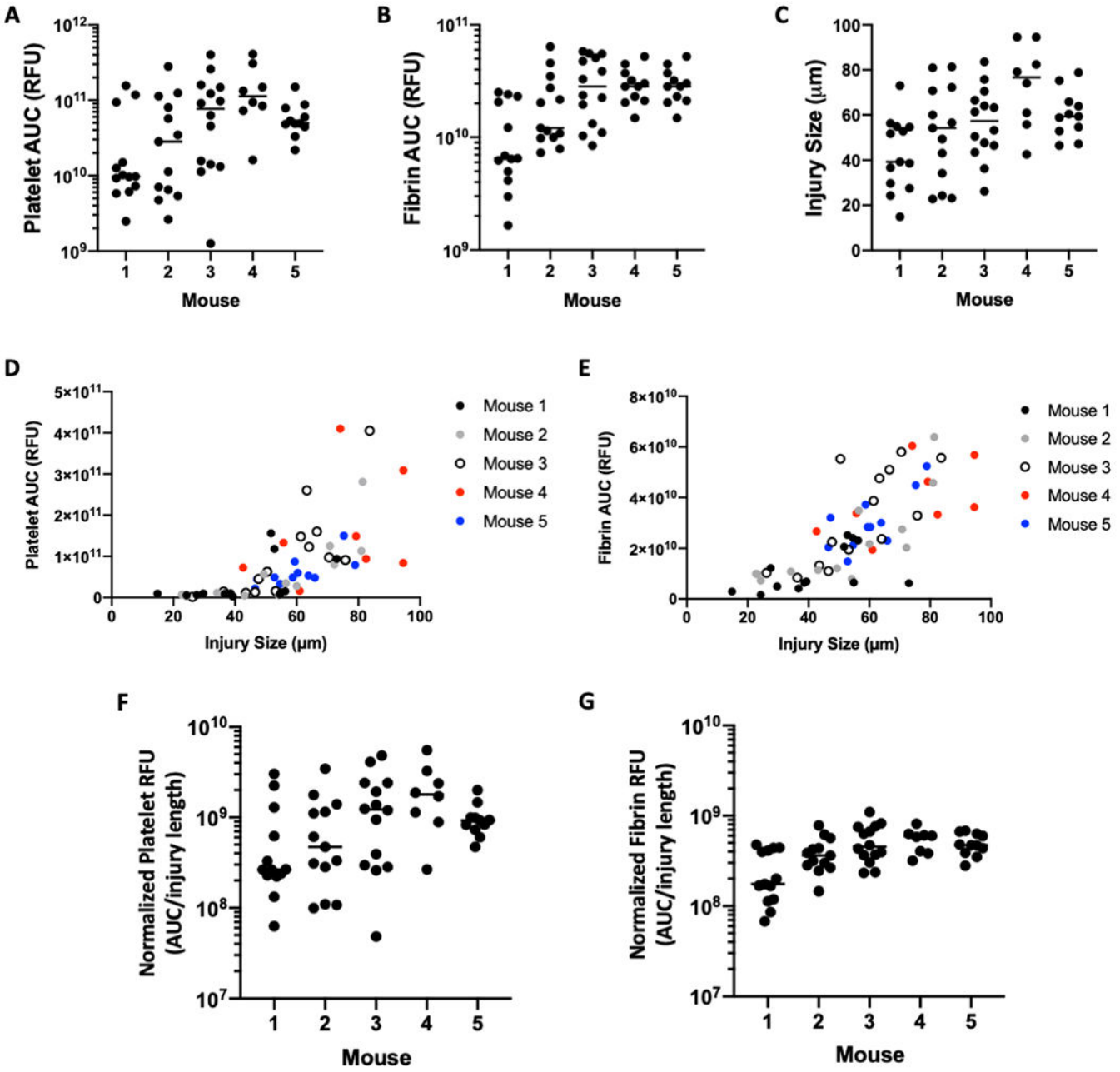

Figure 2: Evaluation of platelet accumulation, fibrin formation, and ablation injury size in genetically identical mice.

(A) Platelet fluorescence (AUC), (B) fibrin fluorescence (AUC), and (C) ablation injury size measurements are shown for the 5 different mice that were used for the evaluation of 59 thrombi presented in Figure 1. Fluorescence values and ablation injury size is plotted for each of the 5 mice to demonstrate the relationship between (D) platelet AUC versus injury size and (E) fibrin AUC and injury size. (F) Platelet fluorescence (corrected AUC) and (G) fibrin fluorescence (corrected AUC) are shown following normalization for injury size. Data represented as individual values with the median.